

Tunnelling in overstressed rock

E. Hoek

Evert Hoek Consulting Engineer Inc., Vancouver, Canada

P.G. Marinos

National Technical University of Athens, Greece

Keynote address presented at EUROCK2009, Dubrovnik, Croatia, 29-31 October 2009.

Published in

Rock Engineering in Difficult Ground Conditions - Soft Rocks and Karst. Vrkljan, I (ed). London: Taylor and Francis Group, 49-60.

COPYRIGHT NOTICE

The following document is subject to copyright agreements

The attached copy is provided for your personal use on the understanding that you will not distribute it and that you will not include it in other published documents.

Tunnelling in overstressed rock

E. Hoek

Evert Hoek Consulting Engineer Inc., Vancouver, Canada

P.G. Marinos

National Technical University of Athens, Greece

ABSTRACT: Overstressing of the rock surrounding a tunnel can result in either brittle fracture of the intact rock or shear failure along pre-existing discontinuities such as joints or shear zones. These two types of failure can co-exist and the extent to which the failures propagate depends upon the characteristics of the rock mass, the magnitude and directions of the in situ stresses, the shape of the tunnel and the intensity and orientation of the discontinuities. Numerical analysis plays an increasingly important role in the assessment of tunnel stability and design of reinforcement and support. Rapid evolution of computer software and hardware offers the potential for the calibration or possible elimination of some of the empirical techniques upon which tunnel designers have to rely.

1 INTRODUCTION

The rock mass surrounding a tunnel can be overstressed when either the intact rock or the discontinuities fail as a result of the stresses induced by the excavation of the tunnel. There are a variety of conditions under which such overstressing can occur and three examples will be discussed in this paper. These are the failure of massive intact rock, sparsely jointed anisotropic rock masses and heavily jointed rock masses. These three cases serve to illustrate the basic principles of assessing the type and extent of failure and of designing reinforcement or support to stabilise the tunnel.

When the conditions for overstressing exist it is seldom possible to prevent failure initiating. When such failure occurs the aim of the design of reinforcement or support is to control the propagation of the failure and to retain the profile of the tunnel. Stability becomes increasingly difficult to control if raveling of the near surface rock pieces is allowed to occur and the interlocking or arching of the rock mass is destroyed by progressive deformation. Support must be chosen to match the deformation characteristics of the rock mass surrounding the tunnel.

2 IN SITU STRESSES

Of all of the quantities that the geotechnical engineer is required to estimate or to measure, the in situ

stress field in a rock mass is one of the most difficult. The vertical stress can be approximated, to an acceptable level of accuracy, by the product of the depth below surface and the unit weight of the rock mass. However, in complex tectonic environments the vertical stresses may be lower (Mayer and Fabre, 1999) or higher (Stille and Palmström, 2008) than the overburden stress. Horizontal stresses of interest to civil and mining engineers are influenced by global factors such as plate tectonics and also by local topographic features.

Zoback (1992) described the World Stress Map project that was designed to create a global database of contemporary tectonic stress data. The data included in this map were derived mainly from geological observations on earthquake focal mechanisms, volcanic alignments and fault slip interpretations. The results included in this map, available at www.world-stress-map.org, are very interesting to geologists involved with regional or continental scale problems. However, other than providing a first estimate of stress directions, they are of limited value to engineers concerned with the upper few hundred metres of the earth's crust. The local variations in the in situ stress field are simply too small to show up on the global scale.

A more useful basis for estimating near-surface horizontal in situ stresses was proposed by Sheorey (1994). He developed an elasto-static thermal stress model of the earth. This model considers curvature of the crust and variations of elastic constants, den-

sity and thermal expansion coefficients through the crust and mantle. A plot of the ratio of horizontal to vertical stress predicted by Sheorey's analysis, for a range of horizontal rock mass deformation moduli, is given in Figure 1. This plot is similar in appearance to that derived by Brown and Hoek (1978) from measured in situ stresses around the world (data points included in Figure 1). While this similarity does not constitute a proof of the correctness of Sheorey's solution, it is at least comforting to find this correlation between theory and observations.

Note that neither Sheorey's equation nor the trends established by Brown and Hoek account for local topographic influences on the stress field. Hence, when making estimates of the in situ stress field in a mountainous area, adjustments must be made to account for these topographic factors. In carrying out an analysis of the stresses induced by the excavation of a tunnel, it is prudent to consider a range of possible in situ stresses. For example, consider a tunnel located in a steep-sided valley where the regional horizontal in situ stress is estimated to be twice the vertical stress. The horizontal stress at right angles to the valley axis could be varied from one half the vertical stress to twice the vertical stress. The stress parallel to the valley could be varied from a minimum value equal to the vertical stress to a maximum value of three times the vertical stress. An exploration of the effects of all possible combinations of these stress values would give a good indication of whether or not these in situ stresses would be critical to the design of the underground excavations. In cases where a preliminary analysis indicates that the design is very sensitive to the in situ stresses, measurement of the in situ stresses has to be considered a priority in the ongoing site investigation and design process.

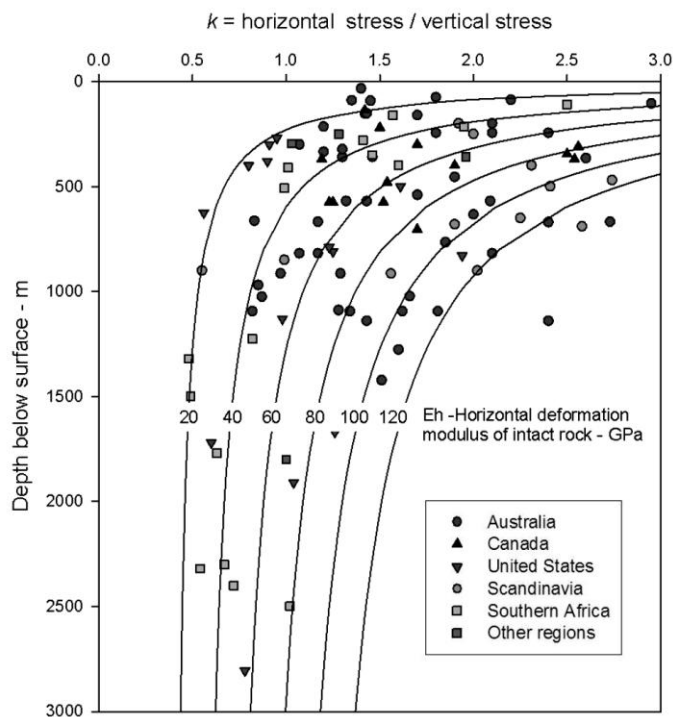


Figure 1. Measured horizontal to vertical stress ratio for various regions around the world compared with theoretical relationships derived by Sheorey (1994).

3 FAILURE OF MASSIVE UNJOINTED ROCK

In massive unjointed rock tensile failure, originating at flaws and defects such as grain boundaries, can occur when the maximum stress on the tunnel boundary exceeds about 40% of the uniaxial compressive strength of the material. These failures propagate along maximum principal stress trajectories and form thin plates parallel to the tunnel boundary as shown in Figure 2. In hard brittle rock, failure of these plates can be associated with significant energy release, which is known as "popping rock", "strainbursts" or, in extreme cases, "rockbursts".



Figure 2. Brittle failure in the walls of a bored vertical shaft in a hard rock deep mine.

Underground hard rock miners have been familiar with this type of failure for many years and there has been considerable research devoted to this problem (Kaiser et al, 1996, Blake and Hedley, 2004). Civil engineers involved in the design of shallow tunnels have paid little attention to this type of failure since it seldom caused major problems. However, with the development of deep level tunnels in mountainous terrain, particularly those driven by tunnel boring machines, there have been an increasing number of brittle failure problems which have raised awareness amongst civil tunnel engineers.

Martin (2008) has shown that tensile cracks initiate at 40 to 50% of the uniaxial compressive strength of most massive rocks, including massive sedimentary rocks. Figure 3 is a plot of crack initiation stresses, determined by strain and acoustic emission measurements, for a wide range of rocks.

In general, brittle failure tends to be self-stabilising when the stresses at the tip of the notch

formed by the failure no longer satisfy the conditions for the failure to propagate. This is shown in Figure 4, based on field observations, in which the depth of brittle failure is plotted as a function of the ratio of maximum boundary stress to uniaxial compressive strength of the intact rock. This plot is useful in that it gives an indication of the volume of rock that has to be supported once the failure has stabilized. As the depth of failure increases, the excavation becomes increasingly difficult to support and the energy release associated with the failure increases.

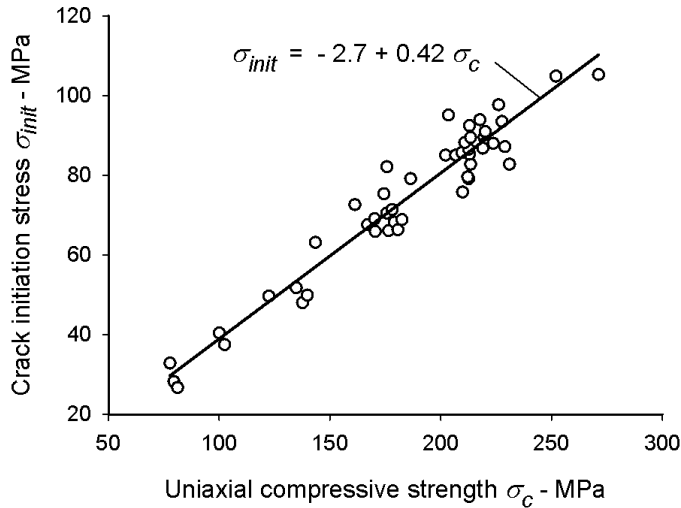


Figure 3. Relationship between brittle crack initiation stress and uniaxial compressive strength of massive rock. After Martin (2008)

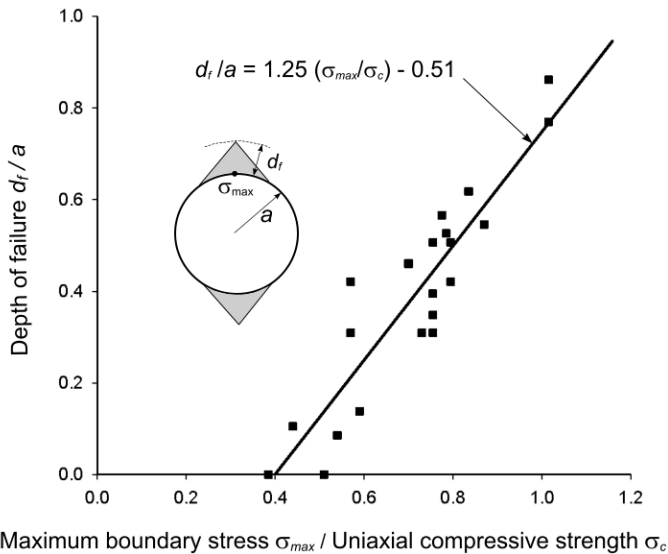


Figure 4: Empirical observations for normalized radius of failure. The standard excavation radius R is calculated from a circle circumscribing a square or horseshoe shaped excavation. The best fit equation is presented in terms of the average uniaxial compressive strength σ_c from laboratory tests. (After Martin et al., 1996).

Figure 5, compiled by Martin et al (1999) from field observations collected by Hoek and Brown (1980) shows the increasing difficulty of stabilising the tunnel as the ratio of maximum boundary stress to uniaxial compressive strength increases. The start

of brittle failure in the bored vertical shaft shown in Figure 2 would correspond to $\sigma_{max}/\sigma_c \approx 0.45$ while the rockburst conditions illustrated in Figure 6 suggest $\sigma_{max}/\sigma_c \approx 1.6$.

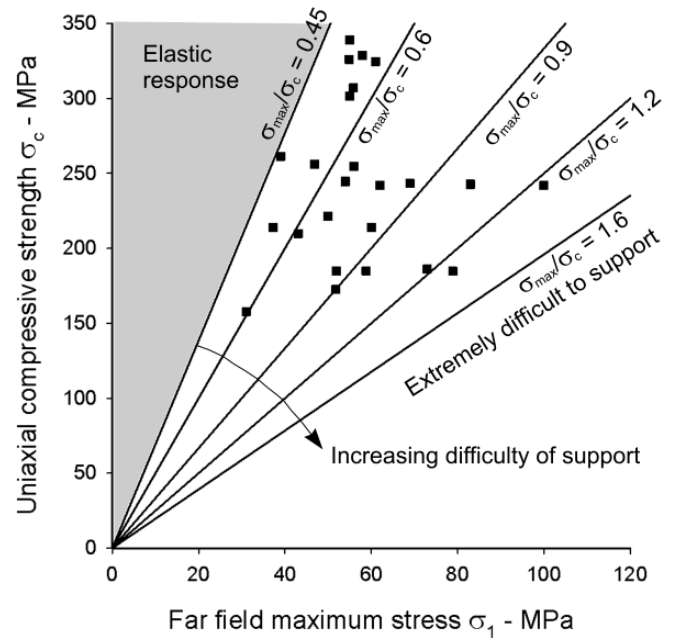


Figure 5. Increasing difficulty of supporting underground excavations with increasing ratio of maximum boundary stress to uniaxial compressive strength (Martin et al, 1999, based on field observations collected by Hoek and Brown, 1980).



Figure 6. Results of a rockburst in a deep level (≈ 3000 m) gold mine in South Africa.

Considerable progress has been made in understanding and predicting the onset of brittle fracture (Martin and Christiansson, 2008, Diederichs et al 2004, Martin 1997) and in the development of empirical depth of failure relationships such as that given in Figure 4 (Martin et al, 1996, Martin et al , 1999).

Reliable numerical models have been developed for predicting the depth, shape and surface extent of brittle failure (Diederichs, 2007). However, these numerical models do not give meaningful predictions of the dilation (bulking) of the fracture zone nor do they explain why very small support pressures can suppress the propagation of failure. With

improvements in computational efficiency and the development of efficient discrete element models it is probable that these limitations will be overcome in time.

The best tools that we have at present are empirical relationships developed by the mining industry (Kaiser et al, 1996). These show that support of tunnels in massive rock, in conditions under which brittle failure can occur, range from light wire mesh and rockbolts, for very minor failure, to heavy support such as the cable lacing illustrated in Figure 7. In such cases early installation of the support, in order to maintain the excavation profile, is essential and the support has to have sufficient ductility to accommodate the volume changes associated with the failure.

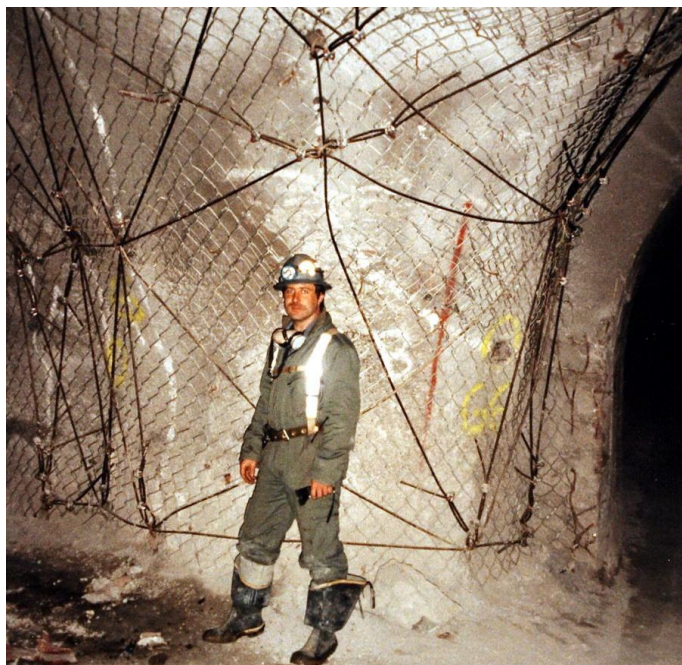


Figure 7. Cable lacing in a hard rock mine in Chile to control damage from brittle failure. Tensioned cables are attached to grouted anchors installed on a regular pattern.

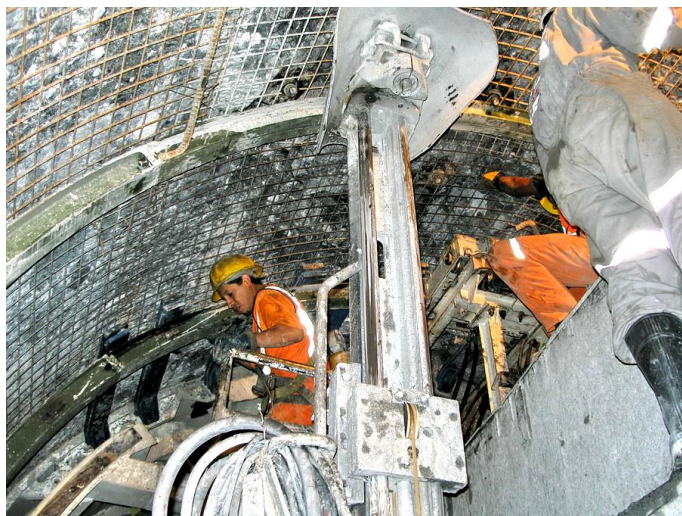


Figure 8. Installation of steel sets immediately behind a TBM shield in the Olmos tunnel in Peru. Photograph provided by R. Guevara (2008).

Figure 8 shows steel sets being installed inside the finger shield, immediately behind the roof shield of an open face hard rock TBM in the Olmos tunnel in Peru. This tunnel is being excavated at depths of up to 2000 m below surface and overstressing in andesitic rock resulting in strainbursting has been controlled by means of the support illustrated (Guevara, 2008). Because of space limitations and the time requirements, it is not practical to install a regular rockbolt pattern immediately behind the TBM and steel sets provide an effective support system.

4 INFLUENCE OF DISCONTINUITIES

The presence of discontinuities (joints, bedding planes, schistosity planes, shear zones etc.) in the rock mass surrounding a tunnel introduces the potential for shear failure along these discontinuities. This depends upon the number, spacing, continuity, orientation and inclination of each discontinuity set as well as the shear strength of the surfaces and the stiffness of the intact rock. For convenience in the following discussion the term "jointed rock mass" will be used to cover all of these discontinuity types.

Apart from those fractures induced by the tunneling process, all the joints in a rock mass are the result of the rock genesis and tectonic deformations during the geological history of the area. Before embarking upon any form of analysis of the behaviour of a jointed rock mass it is necessary to develop a sound geological model and an understanding of the genesis of the joints and of the sequence of their formation (Fookes et al., 2000, Harries and Brown, 2001). This understanding involves input from structural and/or engineering geologists who are familiar with the regional geology and the tectonic history of the area under investigation. Engineers should avoid the temptation to start assigning numbers to the joints or to the rock mass properties until an adequate geological model has been developed.

A full discussion on jointing in rock masses is clearly beyond the scope of this paper. However, in order to provide some guidance, the authors have compiled a matrix of joint characteristics together with other features for typical rocks and this is presented in Appendix 1.

4.1 *Anisotropic failure of sparsely jointed rock*

A sparsely jointed rock mass can be defined as one in which relatively few joint sets occur and where there is frequently a strongly preferred inclination and orientation of the dominant joint set. A typical example would be a bedded sedimentary deposit which has not been subjected to significant post-depositional deformation (a molasse). An example of such a situation is illustrated in Figure 9.



Figure 9: Sandstone and siltstone molasse exposed in the face of a 12 m span tunnel top heading in Greece.

During preliminary site investigations classification systems can be useful in establishing the general characteristics of the rock mass but these classifications, including the GSI system and the associated Hoek-Brown failure criterion (Hoek et al, 2005), are of limited value when highly anisotropic stability problems are anticipated. Under these circumstances there are no short cuts and comprehensive site investigation programs, including establishing the orientation of fractures encountered in diamond drill holes, are required.

Once the geological model has been established and a reasonable understanding of the mechanics of potential failures has been arrived at, a numerical model can be created. This model should incorporate the sequence of excavation and support installation as well as the intact rock and discontinuity characteristics and in situ stresses. Groundwater should be included in the model where this is considered to be significant (Hoek et al, 2008). Fortunately there are a number of commercially available programs which enable users to model all of these features to a level of detail that is acceptable for engineering design.

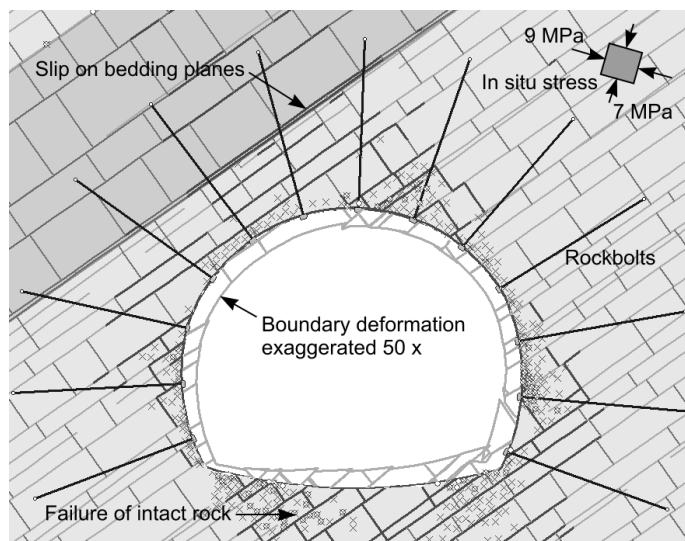


Figure 10. Finite element model of a 12 m span tunnel excavated in interbedded sandstone and siltstone with pre-sheared bedding surfaces.

An example of this type of analysis is shown in Figure 10 in which a 12 m span tunnel is excavated in an interbedded series of sandstone and siltstone layers similar to those illustrated in Figure 9. In this analysis a pattern of 6 m long, 32 mm diameter untensioned grouted rockbolts and wire mesh have been installed 2 m behind the face. A 200 mm thick layer of shotcrete has been installed 5 m behind the face. The procedure for sequencing the installation of reinforcement and support in a two dimensional numerical model is described by Hoek et al (2008).

There is no method for calculating the factor of safety of a tunnel, with a combination of reinforcement and support, such as that shown in Figure 10. As stated earlier, once conditions for failure of either the discontinuities or the intact rock are satisfied it is not possible to prevent this failure. However, the extent of the failure and the tunnel boundary deformations can be controlled by the installation of reinforcement or support. The aim of the designer should be to retain the tunnel profile as far as possible and to prevent or minimise small rockfalls from the surface.

In order to achieve this goal it may be necessary to install a combination of reinforcement and support and to vary the rockbolt length, spacing and inclination to capture specific instability zones. Similarly, the initial and final lining thickness and reinforcement may have to be varied to deal with anisotropic deformation patterns. These changes can only be optimised by iterative analyses with checks to ensure that the factor of safety of each individual support component is within acceptable limits.

4.2 Failure of heavily jointed rock masses

Figures 11 and 12 show examples of heavily jointed rock masses. In Figure 11 the structural pattern of the many joints has been retained while in Figure 12 the fabric has been completely destroyed by tectonic deformation. In either case the joints are sufficiently closely spaced that the rock mass, on the scale of a tunnel, can be treated as isotropic and homogeneous. This greatly simplifies numerical analyses and permits the use of homogeneous models and of rock mass classification schemes to provide input data for rock mass properties.

Another feature of rock masses in which the discontinuities have been pre-sheared by tectonic deformation is that they have a limited capacity to sustain shear stresses. Consequently, over geological time, the in situ stresses tend to equalise and a reasonable first approximation of the in situ stress field is that horizontal and vertical stresses are equal. This conclusion is generally impossible to confirm by direct measurement but back analysis of the behaviour of tunnels excavated in such materials tends to confirm this equalisation of the in situ stresses.



Figure 11. Heavily jointed andesite in an excavated slope face in Papua New Guinea.

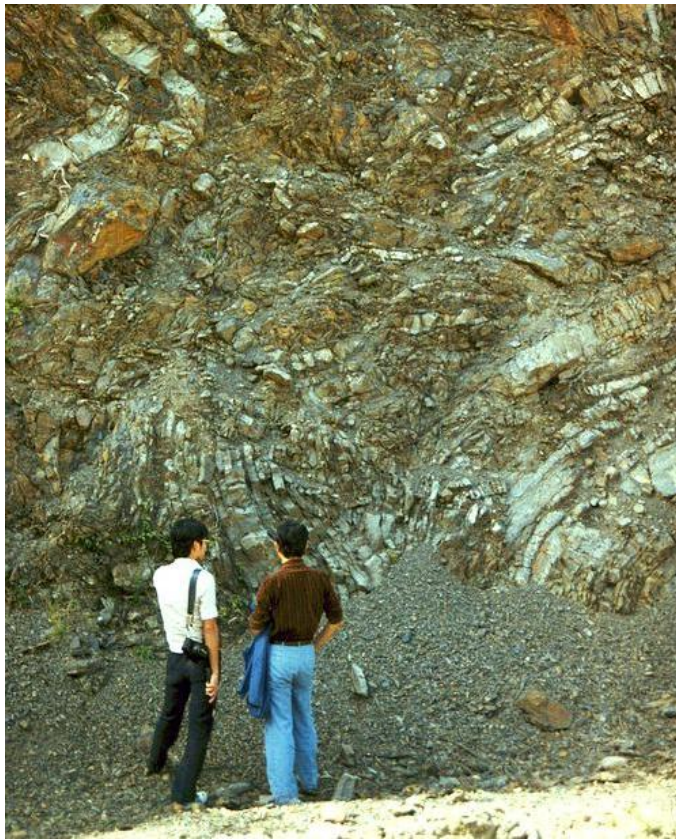


Figure 12: Destruction of structural fabric as a result of tectonic deformation of an interbedded sedimentary rock mass in southern Taiwan.

Figure 13 gives a comparison between finite element analyses of a tunnel excavation using a heavily jointed model (on the left) and an equivalent homogeneous model (on the right). The jointed model has

the advantage that structural data on jointing obtained in the field and laboratory data on rock mass properties can be used directly in the model. However, the computational demands of such models limit their current use to relatively simple problems. On the other hand, the equivalent homogeneous model allows for very efficient numerical modelling but it imposes significant demands on the user to estimate realistic material properties.

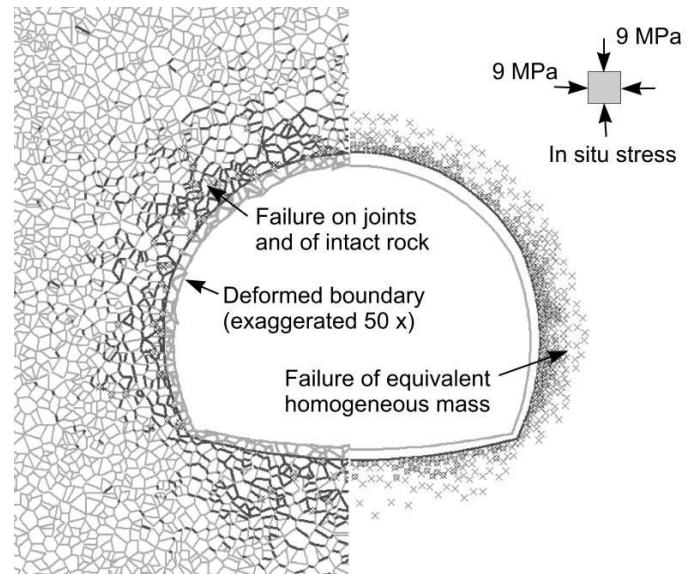


Figure 13. Comparison between results of analyses using a two dimensional continuum model with closely spaced Voronoi joints (left) and equivalent rock mass properties (right). Note that intact properties are used for the rock pieces between joints in the jointed model. Phase2 v7 model (www.rocscience.com).

4.3 Inclusion of joints in numerical models

Several commercially available continuum models permit the insertion of individual joints or joint networks (Rocscience, 2008, Lorig, 2007). These networks may include parallel or cross-jointed arrays, joints with a statistically distributed finite trace length (Baecher et al 1978), Veneziano or Voronoi joints patterns (Dershowitz, 1985). These models make it possible to study the behaviour of a wide variety of heavily jointed rock masses and they have proved to be very useful for practical tunnel designs.

In using these continuum models it has to be kept in mind that they do not permit separation of joint planes or rotation of blocks and that their use should be restricted to small deformation problems. However, since most tunnel designers are interested in limiting the deformation of tunnels and in maintaining the opening profile, this restriction is not a serious limitation in tunnel design.

For larger deformation problems where joint separation and block failure and rotation are likely to occur, discrete element (Lorig, 2007) or combined finite-discrete element models (Munjiza, 2004, Crook et al, 2003) need to be used. Some of these

codes were developed for applications other than rock engineering and need some adaptation before they can be used efficiently for tunnel design.

These are sophisticated and powerful codes and the potential user should not under-estimate the investment in time and resources required in order to learn to utilise them correctly. For research or consulting groups interested in remaining in the forefront of tunnel design this investment is well worth making.

4.4 Use of rock mass classifications

The use of rock mass classification systems goes back more than 60 years when authors like Terzaghi (1946) attempted to describe the characteristics of rock masses and their response to tunnelling. Since that time numerous rock mass classifications have been developed and probably the best known are those of Barton et al (1974) and Bieniawski (1976). These classification systems played an important role in tunnel design before the development of the numerical models discussed above. They continue to play an important role in providing initial estimates of the range of problems likely to be encountered and of solutions that can be considered and also in estimating rock mass properties for input into numerical models.

Hoek and Brown (1980) considered that more detailed rock mass property information would be required as numerical modelling became more readily available and more widely used in design. They set out to develop a failure criterion (the Hoek-Brown criterion) and a classification system (The Geological Strength Index, GSI) specifically for this purpose (Hoek and Marinos, 2007). This classification differs from those described above in that it has no end use other than to provide input for the Hoek-Brown criterion. It was not intended for and should not be used for estimating tunnel support requirements, excavation advance rates or tunnel costs. Furthermore, it assumes a homogeneous isotropic rock mass and should not be used for the analysis of anisotropic or strongly structurally controlled rock mass behaviour.

An example of the application of the GSI classification and the Hoek-Brown criterion has been published by Hoek and Guevara (2009). This deals with the Yacambú-Quibor tunnel in Venezuela in which severe squeezing was encountered in graphitic phyllite at depths of up to 1200 m below surface. The analysis utilises a relationship developed by Hoek and Marinos (2000) for the prediction of the extent of squeezing on the basis of the ratio of rock mass strength σ_{cm} to overburden stress p_o , shown in Figure 14.

Figure 15 shows that there are a significant number of locations along the tunnel where the strain approaches or exceeds 10% which, according to Figure 14, represents a severe squeezing condition.

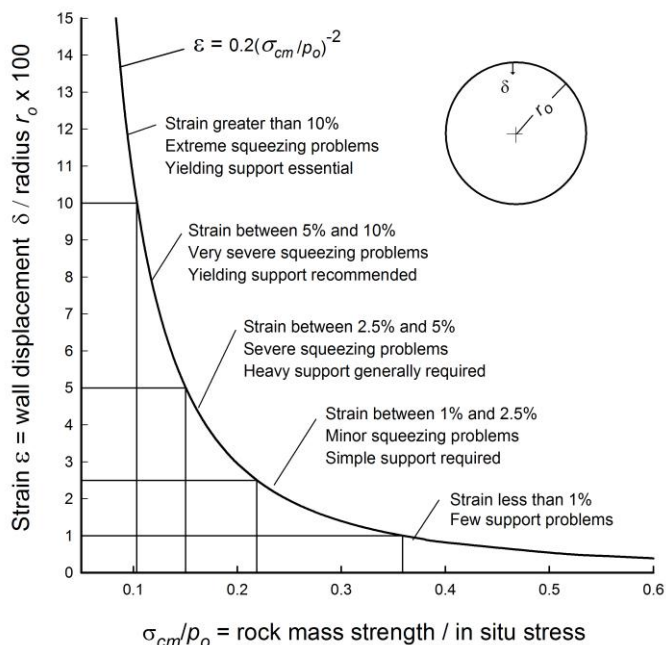


Figure 14: Relationship between tunnel strain and ratio of rock mass strength to in situ stress (Hoek and Marinos, 2000).

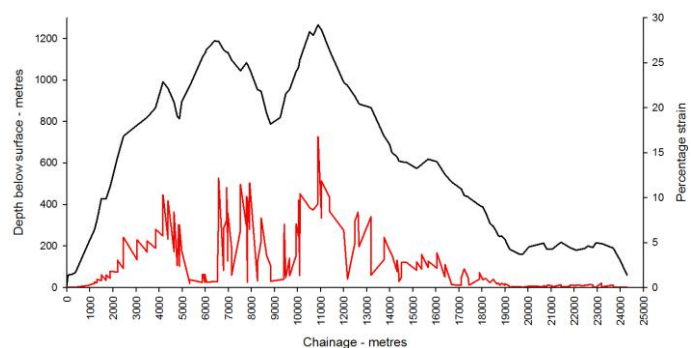


Figure 15: Strain along the Yacambú-Quibor tunnel predicted from the ratio of rock mass strength to in situ stress. (Hoek and Guevara, 2009).



Figure 16: Failure of a tunnel section due to very severe squeezing (background) and re-mined and re-supported tunnel (foreground).

During excavation of the tunnel severe squeezing was encountered in a number of the locations where inadequate support had been installed. Re-mining and rehabilitation was required in these locations as illustrated in Figure 16. Lessons learned in such cases were used to develop a support design procedure based on the use of sliding joints in circular steel sets. These sets were installed as close as possible to the excavated face and the 5 m diameter tunnel was permitted to converge about 50 cm before the sliding joints locked and the sets developed their full capacity. At a distance of about 15 m behind the face the shotcrete windows, that had been left to permit the joints to slide, were filled and additional shotcrete was applied to build up a final lining of up to 70 cm thickness, depending on the rock mass properties and in situ stress levels.

5 PREDICTIONS FOR THE FUTURE

Rock engineers have to work within the limitations of available technology and, without doubt, some of the most severe limitations are associated with the estimation of rock mass properties. The strength and deformation characteristics of the rock and the discontinuities play a major role in determining stability as well as the reinforcement and support requirements in tunnelling,

Efforts to overcome these limitations have resulted in tools such as the GSI classification (Hoek and Marinos, 2008) which, at best, can only be regarded as crude interim solutions. It is simply not possible, within the constraints of a classification system based on a limited number of estimated input parameters, to capture the actual behaviour of heterogeneous rock masses. This is not to say that these efforts have not been useful since, when they were developed, there very few practical alternatives available.

Fortunately, with developments in computer hardware and software technology, there is now a reasonable expectation that some of mysteries of rock mass property estimation may be dispelled over the next decade. This expectation is centred on our rapidly improving ability to incorporate laboratory determined intact rock and discontinuity properties into numerical models. As discussed in Section 4.3 above, several commercially available codes permit this type of analysis and some of them are capable of producing credible results in the analysis of failure initiation and post failure behaviour of complex rock mass and applied stress conditions (Lorig, 2007).

Discrete element and combined finite-discrete element analyses are currently fashionable research topics and geotechnical journals and conferences abound with papers with spectacular demonstrations of fractured rock masses falling apart. Very few of these techniques are available as robust, validated

and user-friendly tools that the average tunnel designer could use. As with the development of other numerical tools, several years will be required to sort the wheat from the chaff and to allow a consolidation of the technology. Eventually these methods will be integrated into existing software or they will form the basis of a new family of powerful two- and three-dimensional design tools.

The authors look forward to the time when these numerical tools will allow us to at least calibrate if not replace completely some of the empirical methods, such as the GSI classification and the Hoek – Brown criterion that we use today.

6 REFERENCES

- Barton, N.R., Lien, R. and Lunde, J. 1974. Engineering classification of rock masses for the design of tunnel support. *Rock Mech.* **6**(4), 189-236
- Baecher, G.B., Lanney, N.A. and H.H. Einstein. 1978. Statistical Description of Rock Properties and Sampling. *Proceedings 18th U.S. Symposium on Rock Mechanics*, 5C1-8.
- Bieniawski Z.T. 1976. Rock mass classification in rock engineering. *In Exploration for Rock Engineering*, Proc. of the Symp., (ed. Z.T. Bieniawski) 1, 97-106. Cape Town, Balkema.
- Blake, W. and Hedley, D.F.G. 2004. *Rockbursts: Case Studies from North American Hard-Rock Mines*. New York: Society for Mining, Metallurgy, and Exploration. 121 p.
- Brown, E.T. and Hoek, E. 1978. Trends in relationships between measured rock in situ stresses and depth. *Int. J. Rock Mech. Min. Sci. & Geomech. Abstr.* **15**, 211-215.
- Crook, A, Wilson, S., Yu, J. G and Owen, R. 2003, Computational modelling of the localized deformation associated with borehole breakout in quasi-brittle materials. *J. Petroleum Science and Engineering* **38**, 177– 186.
- Diederichs, M. S. 2007. Mechanistic interpretation and practical application of damage and spalling prediction criteria for deep tunnelling. *Can. Geotech. J.*, **44**, 1082-1116.
- Diederichs, M.S., Kaiser, P.K. and Eberhard, K.E. 2004. Damage initiation and propagation in hard rock and influence of tunnelling induced stress rotation. *Int. J. Rock Mech. Min. Sci.*, **41**: 785-812.
- Dershowitz, W. 1985. Rock Joint Systems. *Ph.D. Thesis*, Massachusetts Institute of Technology, Cambridge, MA.
- Fookes, P., Baynes, Fr. and Hutchinson, J. 2000. Invited Keynote Lecture: Total geological history: a model approach to the anticipation, observation and understanding of site conditions. *In Proceedings of GeoEng2000*, Melbourne, Technomic Publ. Co, Lancaster, Pennsylvania, 370-459
- Guevara, R. 2008. Personal Communication.
- Harries, N.J. and Brown, E.T. 2001. Hierarchical modelling of rock mass discontinuities. *Proceedings of the ISRM Regional Symposium Eurock 2001*, Espoo, Finland. London, Taylor & Francis. 243-248.
- Hoek, E and Marinos, P. 2000, Predicting tunnel squeezing problems in weak heterogeneous rock masses. *Tunnels and Tunnelling International*, Part 1, **32**(11), 45-51; Part 2, **32**(12), 33-36
- Hoek, E and Marinos, P. 2007. A brief history of the development of the Hoek-Brown failure criterion. *Soils and Rocks*, No. 2. November 2007.
- Hoek, E. and Brown, E.T. 1980. *Underground excavations in rock*. London: Inst. Mining and Metallurgy.

- Hoek, E., Carranza-Torres, C., Diederichs, M.S. and Corkum, B. 2008. Integration of geotechnical and structural design in tunnelling. *Proceedings University of Minnesota 56th Annual Geotechnical Engineering Conference*. Minneapolis, 29 February 2008, 1-53.
- Hoek, E., Marinos, P and Marinos, V. 2005. Characterization and engineering properties of tectonically undisturbed but lithologically varied sedimentary rock masses, *International Journal of Rock Mechanics and Mining Sciences*, **42**(2), 277-285.
- Hoek, E. and Guevara, R. 2009. Overcoming squeezing in the Yacambú-Quibor Tunnel, Venezuela. *Rock Mech. & Rock Eng.* **42**(2), 389-418.
- Kaiser P.K., McCreath D.R. and Tannant D.D. 1996. *Canadian Rockburst Support Handbook*. Canadian Rockburst Research Program, Vol II, Book I (1990-1995). CAMIRO Mining Division. 343 p.
- Kaiser, P.K., Diederichs, M.S., Martin, D., Sharpe, J. and Steiner, W. 2000. Invited Keynote Lecture: Underground Works in Hard Rock Tunnelling and Mining. In *Proceedings of GeoEng2000*, Melbourne, Technomic Publ. Co, Lancaster, Pennsylvania, 841-926
- Lorig, L. 2007. Using numbers from geology. *Proc. 11th Congress of the ISRM*. London: Taylor and Francis. 1369-77.
- Martin, C. D.; Kaiser, P. K. & Alcott, J. M. 1996. Predicting the depth of stress-induced failure around underground openings. In *Proc. 49th Canadian Geotechnical Conference*, St. John's, C-CORE, Vol 1, 105-114
- Martin, C. D. 1997. The effect of cohesion loss and stress path on brittle rock strength. *Can Geotech J*, **34**(5):698-725.
- Martin, C.D., Kaiser, P.K., & McCreath, D.R. 1999. Hoek-Brown parameters for predicting the depth of brittle failure around tunnels. *Can. Geotech. Jour.*, **36** (1): 136-151.
- Martin, C.D. and Christiansson, R. 2009, Estimating the potential spalling around a deep nuclear waste repository in crystalline rock. Accepted for publication in *Int. J. Rock Mech. Min. Sci.* **46**(2), 219-228.
- Martin, D. 2008. Personal communication.
- Marinos, P., Marinos, V. and Hoek, E. 2007. Geological Strength Index (GSI). A characterization tool for assessing engineering properties for rock masses. *Underground Works under Special Conditions*, Romana, Perucho, Olalla edit., Francis and Taylor, 13-21
- Mayeur, B. and Fabre, D. 1999. Mesure et modélisation des contraintes naturelles. Application au projet de tunnel ferroviaire Maurienne-Ambin. *Bull. Eng. Geol. & Env.*, **58**, 45-59.
- Munjiza. A. 2004. *The Combined Finite-Discrete Element Method*. Chichester: Wiley & Sons. 333 p.
- Rocscience Inc. 2008 Phase2 7.0: Expanding the Frontiers of Geotechnical Engineering. www.rocscience.com, Toronto, Ontario, Canada.
- Sheorey, P.R. 1994. A theory for in situ stresses in isotropic and transversely isotropic rock. *Int. J. Rock Mech. Min. Sci. & Geomech. Abstr.* **31**(1), 23-34.
- Stille, H. and Palmström, A. 2008. Ground behaviour and rock mass composition in underground excavations. *Tunnelling and Underground Space Technology*, **23**, 46-64.
- Terzaghi, K. 1946. Rock defects and loads in tunnel supports. *Rock tunnelling with steel supports*. R.V. Proctor and T.L. White, eds., The Commercial Shearing and Stamping Co., Youngstown, Ohio, 17-99.
- Zoback, M.L. 1992. First- and second-order patterns of stress in the lithosphere: the World Stress Map Project. *Journal of Geophysical Research*. **97**(B8), 11761-11782.

The authors of this paper have always advocated that users of the GSI classification should rely on the application of sound engineering geology principles rather attempt to be too quantitative in the estimation of rock mass properties. In the introductory box of the GSI chart, a typical example of which is given in Table 1, they warn: “Do not attempt to be too precise. Quoting a range of GSI of 33 to 37 is more realistic than giving GSI = 35.”

One of the typical problems faced by inexperienced users is to judge the properties of the rock and the discontinuities in a specific rock mass. Even geologists will sometimes fail to recognise the engineering significance of their interpretation of the rock mass characteristics. A discussion on the applications of GSI can be found in Marinos et al (2007).

In an attempt to provide some ideas on the choice of the properties that should be used in working with the GSI charts, a new pair of tables are presented in this appendix. Table 2 give a number of possible combinations of properties that may occur in different rock types. Table 3 defines these properties for intact rock, joints and for rock masses. The properties considered include intact strength, alteration, weathering, solution potential, anisotropy, joint characteristics and permeability.

For example, serpentinite would be categorised as follows:

Dominant factors

- 1B-C: UCS ranges from 15 to 100 MPa
- 3D: High weathering potential
- 8C-D: Planar to very planar joints
- 9D: Possibility of clay filling in joints
- 10D: Potential for heavy slickensided joints
- 11A-C: Generally low joint controlled permeability

Significant factors

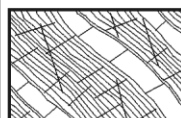
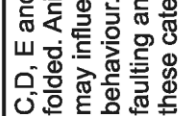
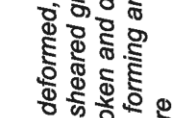
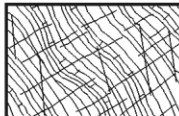
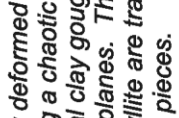
- 2B-C: Slight to moderate alteration potential
- 7B: Slight anisotropy
- 13B: Slight persistent schistosity when tectonised
- 4B: Slight swelling potential

Factors that can be ignored

- 5A: No solution potential
- 6A: No potential for void formation
- 12A: No persistent thin bedding planes
- 14A: No heterogeneity due to alternating layers

Note: The combinations included in the Table 2 are those found most frequently in rock and rock masses in situ depending from their petrographic nature and tectonic history. Other combinations may occur.

Table 1- Geological Strength Index Table for graphitic phyllite

<p>GSI FOR PHYLLITES AT YACAMBU-QUIBOR (After Marinós, P and Hoek, E, 2000)</p> <p>From a description of the lithology, structure and surface conditions (particularly schistosity planes), choose a box in the chart. Locate the position in the box that corresponds to the condition of the discontinuities and estimate the average value of GSI from the contours. Do not attempt to be too precise. Quoting a range from 33 to 37 is more realistic than giving GSI = 35. Note that the Hoek-Brown criterion does not apply to structurally controlled failures. Where unfavourably oriented continuous weak planar discontinuities are present, these will dominate the behaviour of the rock mass. The strength of some rock masses is reduced by the presence of groundwater and this can be allowed for by a slight shift to the right in the columns for fair, poor and very poor conditions. Water pressure does not change the value of GSI and it is dealt with by using effective stress analysis.</p> <p>COMPOSITION AND STRUCTURE</p>	<p>SURFACE CONDITIONS OF DISCONTINUITIES (Predominantly schistosity planes)</p>	<p>VERY GOOD - Very rough, fresh unweathered surfaces</p>	<p>GOOD - Rough, slightly weathered surfaces</p>	<p>FAIR - Smooth, moderately weathered and altered surfaces</p>	<p>POOR - Very smooth, occasionally slickensided surfaces with compact coatings or fillings with angular fragments</p>	<p>VERY POOR - Very smooth slickensided or highly weathered surfaces with soft clay coatings or fillings</p>
<p>A. Thick bedded silicified phyllite. The effect of weak coatings on the discontinuity planes is minimized by the confinement of the rock mass. In shallow tunnels or slopes these planes may cause structurally controlled instability.</p> 	<p>E. Weak graphitic phyllite with silicified layers</p> 	<p>70</p>	<p>60</p> <p>A</p>	<p>50</p> <p>B C D</p> <p>40</p>	<p>E</p>	<p>F</p> <p>20</p>
<p>B. Silicified with thin layers of graphitic phyllite</p> 	<p>D. Graphitic phyllite with silicified phyllite and chert layers</p> 	<p>30</p>	<p>F</p>	<p>G</p>	<p>H</p>	<p>10</p>
<p>C. Silicified & graphitic phyllite in similar amounts</p> 	<p>F. Tectonically deformed, intensively folded/faulted, sheared graphitic phyllite with broken and deformed silicified layers forming an almost chaotic structure</p> 	<p>20</p>	<p>F</p>	<p>G</p>	<p>H</p>	<p>10</p>
<p>C, D, E and G - may be more or less folded. Anisotropy due to schistosity may influence the stress dependent behaviour. Tectonic deformation, faulting and loss of continuity moves these categories to H and F.</p> 	<p>H. Tectonically deformed graphitic phyllite forming a chaotic structure with occasional clay gouge on intense shear planes. Thin layers of silicified phyllite are transformed into small rock pieces.</p> 	<p>10</p>	<p>H</p>	<p>G</p>	<p>H</p>	<p>10</p>

↑ : Means deformation after tectonic disturbance

Table 2 – Possible features for different rock types

Rock type	Class	Group	Texture			
			Coarse	Medium	Fine	Very fine
SEDIMENTARY	Clastic		Conglomerates Breccias 1B-D, 2A, 3B-C, 4A, 5B, 6B, 7A, 8B, 9BC, 10B, 11A, 12A-B, 13A, 14C	Sandstones 1A-B, 2A, 3B-C, 4A, 5A, 6A, 7A, 8A, 9B, 10B, 11A, 12B, 13A, 14D	Siltstones 1C-D, 2A, 3B, 4A-B, 5A, 6A, 7A, 8C, 9D, 10D, 11D, 12C, 13A, 14D	Claystones - Marls 1D, 2B, 3B-C, 4B-C, 5A, 6A, 7A, 8D, 9D, 10D, 11D, 12B, 13A, 14D
						Shales 1D, 2B, 3B-C, 4B-C, 5A, 6A, 7C-D, 8D, 9D, 10D, 11D, 12D, 13D, 14A
	Non-Clastic	Carbonates	Limestones – Dolomites 1B-C, 2A, 3A, 4A, 5A, 6D, 7A, 8B, 9A, 10B, 11A, 12A, 13A, 14C			
		Evaporites	Gypsum 1C, 2A, 3B, 4B, 5D, 6D, 7A, 8C, 9?, 10C, 11A, 12A, 13A, 14C	Anhydrite 1C, 2A, 3D, 4D, 5B, 6B, 7A, 8C, 9?, 10C, 11D, 12A, 13A, 14A		
METAMORPHIC	Non Foliated		Marble 1B, 2A, 3A, 4A, 5A, 6D, 7B, 8B, 9A, 10B, 11A, 12B, 13A, 14C	Hornfels (or cherts in sedimentary rocks) 1A, 2A, 3A, 4A, 5A, 6A, 7A, 8B, 9A, 10B, 11A, 12C, 13A, 14D		Quartzite 1A, 2A, 3B, 4A, 5A, 6A, 7B, 8A, 9B, 10B, 11A, 12B, 13C, 14D
			Slightly Foliated	Amphibolites – Gneiss 1A, 2B, 3C-D, 4A, 5A, 6A, 7C 8A, 9C-D, 10C, 11A, 12A, 13A, 14A		
	Foliated	Micaschists 1A, 2B, 3B-C, 4A, 5A, 6A, 7C, 8B, 9C-D, 10C, 11A, 12B, 13C, 14C	Phyllites 1C, 2B-C, 3C-D, 4B, 5A, 6A, 7D, 8D, 9C-D, 10D, 11C, 12C, 13D, 14D			
IGNEOUS	Plutonic	Light	Granite - Diorite – Granodiorite 1A, 2C, 3D, 4A, 5A, 6A, 7A, 8A, 9C, 10B-C, 11A, 12A, 13A, 14A			
		Dark	Gabbro - Norite 1A, 2C, 3C, 4A, 5A, 6A, 7A, 8A, 9C, 10C, 11A, 12A, 13A, 14A			
	Hypabyssal	Peridotite 1A, 2C-D, 3D, 4A, 5A, 6A, 7A, 8B, 9C-D, 10C, 11A, 12A, 13A, 14A	Serpentinites 1B-C, 2B-C, 3D, 4B, 5A, 6A, 7B, 8C-D, 9D, 10D, 11A-C, 12A, 13B, 14A			
	Volcanic	Lava	Rhyolite – Dacite – Andesite 1A, 2C, 3B-C, 4A, 5A, 6B, 7A, 8A, 9C, 10C, 11A, 12A, 13A, 14A	Basalt 1A, 2A-B, 3A-B, 4A, 5A, 6A, 7A, 8B, 9B-C, 10B, 11A, 12A, 13A, 14A		
		Pyroclastic	Agglomerate – Volcanic Breccia 1B-C, 2C, 3C, 4B-D, 5A, 6B, 7A, 8A, 9C, 10B, 11A, 12A, 13A, 14C	Tuff 1C-D, 2D, 3D, 4B-C, 5A, 6B, 7A, 8B, 9C, 10C, 11A, 12A, 13A, 14D		

For definitions of 1,2,..., A, B,..., refer to table 3.

Note: The combinations included in the table are those found most frequently in rock and rock masses in situ depending from their petrographic nature and tectonic history. Other combinations may occur in some cases except if not applicable (N/A) is noted (see table 3). This table is for guidance only and it should not be used as a substitute for site observations and data acquisition from a site investigation program.

Table 3 – Definition of rock type features

Property		A	B	C	D	
UCS of sound intact material	1	Very high > 100 MPa	High 50 -100 MPa	Medium 15 - 50 MPa	Low < 15 MPa	Intact Rock
Alteration potential	2	None	slight	moderate	high	
Weathering potential	3	None	slight	moderate	high	
Swelling potential	4	N/A	slight	moderate	high	
Solution potential	5	N/A	slight	moderate	high	
Voids – potential for formation	6	N/A	possible		Yes	
Anisotropy of intact rock	7	None	slight	moderate	high	
Joint surface characteristics (excluding schistosity)	8	very rough	waviness	planar with slight waviness	very planar	Joints
Joint infilling from crushed rock – excluding excavation damage	9	None	Sandy	Clay with sandy particles	Clay	
Slickensided joints – potential in sheared rock	10	None	minimal	moderate	heavy	
Permeability or rock mass	11	Depending on jointing or karstification	-	Low	Very Low	Rock mass
Persistent thin bedding planes	12	None	possible	frequent	In most cases	
Persistent schistosity	13	N/A	slight	moderate	high	
Heterogeneity - Possibility of alternating weak and strong rock layers on the scale of the engineering structure	14	No	-	Rare	Yes	